

Journal Pre-proof

Injectable hydrogel-based drug delivery system for cartilage regeneration

Luis García-Fernández, Marta Olmeda-Lozano, Lorena Benito-Garzón, Antonio Pérez-Caballer, Julio San Román, Blanca Vázquez-Lasa



PII: S0928-4931(19)34050-0

DOI: <https://doi.org/10.1016/j.msec.2020.110702>

Reference: MSC 110702

To appear in: *Materials Science & Engineering C*

Received date: 4 November 2019

Revised date: 18 December 2019

Accepted date: 27 January 2020

Please cite this article as: L. García-Fernández, M. Olmeda-Lozano, L. Benito-Garzón, et al., Injectable hydrogel-based drug delivery system for cartilage regeneration, *Materials Science & Engineering C* (2020), <https://doi.org/10.1016/j.msec.2020.110702>

This is a PDF file of an article that has undergone enhancements after acceptance, such as the addition of a cover page and metadata, and formatting for readability, but it is not yet the definitive version of record. This version will undergo additional copyediting, typesetting and review before it is published in its final form, but we are providing this version to give early visibility of the article. Please note that, during the production process, errors may be discovered which could affect the content, and all legal disclaimers that apply to the journal pertain.

© 2020 Published by Elsevier.

Injectable Hydrogel-Based Drug Delivery System for Cartilage Regeneration

Luis García-Fernández^{a,b}, Marta Olmeda-Lozano^c, Lorena Benito-Garzón^d, Antonio Pérez-Caballer^{c,e}, Julio San Román^{a,b}, Blanca Vázquez-Lasa^{a,b}*

In memoriam: This paper is dedicated to the memory of José Antonio de Pedro Moro, University of Salamanca, who participated in the beginning of the work and was dead 25th February 2016.

^a Biomaterials Group/Institute of Polymer Science and Technology, Spanish National Research Council (ICTP-CSIC), Madrid 28006, Spain

^b Centro de Investigaciones Biológicas en Red, Bioingeniería, Biomateriales y Nanomedicina (CIBER-BBN), Madrid 28029, Spain

^c University Hospital Infanta Elena, Valdemoro 28342, Spain

^d Faculty of Medicine, University of Salamanca, Salamanca 37007, Spain

^e Faculty of Health Science, University Francisco de Vitoria, Pozuelo de Alarcón 28223, Spain

* Corresponding author: luis.garcia@csic.es

Keywords: Cartilage regeneration, osteoarthritis, injectable hydrogel, hyaluronic acid, gelatin.

1. Introduction

Osteoarthritis (OA) is a chronic degenerative disease of slow progression that affects the hip, knee, distal phalangeal and intervertebral joints. It is characterized by joint pain, accentuated sensitivity, rigidity and alteration in mobility [1]. The disorder first manifests at the molecular and cellular level (abnormal metabolism of the tissues of the joint) followed by anatomical or physiological alterations (degradation and loss of cartilage, bone remodeling, osteophyte formation, synovial inflammation, sclerosis and loss of subchondral bone). The commitment of the hip and knees are a common cause of disability. OA is a severe clinical and public health problem, close to 50% of the people suffered OA at different levels, but the current clinical treatments available are incapable to reverse disease progression [2].

The most used current treatment are oral medications with nonsteroidal anti-inflammatory drugs (NSAID) or corticoids, but these treatments cause different adverse effects, such as gastrointestinal reactions or renal dysfunction [2]. In the case of severe OA (debilitating pain, major functional limitation) is necessary the use of surgery. Currently, the regeneration of cartilage tissue is under research without found clinical satisfactory solutions [3]. The technique of microfracture is the clinical procedure most widely used to treat cartilage injury [4]. This technique consists in perforate the subchondral bone, allowing the bleeding and the formation of a clot rich in growth factor and mesenchymal cells [4, 5]. The cartilage regenerated by this technique is a fibrocartilage, which presents worst physical properties than the original one and has problems of integration with the surrounding tissue.

Due to the different problems on surgery-based techniques for the treatment of osteoarthritis, other different methods are under study. In this sense, hydrogels are one of the emergent candidates in cartilage regeneration. The use of hydrogel has several

advantages compared to the use of other techniques. The use of natural or bio-inspired polymers for the synthesis of hydrogels allows the preparation of scaffolds with properties close to the native extracellular matrix (ECM) [6]. Another advantage is the possibility of making them injectable and allows us to use a non-invasive approach [7]. Different examples of natural polymers are hyaluronic acid, collagen, gelatin, alginate, chitosan, chondroitin sulfate and fibrin. On the other hand, semi-interpenetrating networks (semi-IPN) hydrogels mimicking ECM features have been proposed for cartilage regeneration. These systems present the advantages of possessing improved properties and synergistic effects respect to the individual polymers [8]. Pescosolido *et al.* reported the suitability of hyaluronic acid/dex-HEMA semi-IPNs for encapsulating chondrocytes to manufacture bioprinted constructs for tissue engineering [9]. Other authors proposed the use of semi-IPN hydrogels of oxidized dextran/amino gelatin and hyaluronic acid cell transplantation [10].

In this work, we developed an injectable semi-IPN hydrogel based on gelatin and hyaluronic acid (HA). Gelatin is produced by partial hydrolysis of collagen and promotes cell adhesion, proliferation, migration and differentiation due to the presence of RGD sequence on its structure [11]. Hyaluronic acid is a non-sulfated glycosaminoglycan and one of the major components of the ECM [12]. HA is involved in diverse biological processes, i.e. proteoglycan (PG) organization, tissue hydration or cell differentiation [13]. The application of a semi-IPN hydrogel system able to in situ release HA to the injured cartilage would contribute with some advantages. HA demonstrated to improve the synthesis of chondroitin-6-sulfate, collagen II, aggrecan and DNA [14]

There are different ways of crosslinking hydrogels; the most common are the use of physical crosslinker [15], chemical crosslinker [16], Michael-type conjugate addition

reaction [17] or Schiff-base formation [18]. In most of the cases, the use of chemical initiators may promote toxicity and cell death on injectable hydrogels [19]. In the last decade, a novel methodology without chemical initiators was developed. This technique involves the partial oxidation of polysaccharides to obtain a reactive polymer that can interact with amine groups of other natural polymers [20]. In particular, oxidized dextran demonstrated to act as macromolecular crosslinker for polymers bearing amino groups to formulate crosslinked hydrogels for cartilage tissue engineering [21] [22].

In this work, we report the synthesis of an injectable and biodegradable drug delivery system from oxidized dextran (Dex-ox), gelatin and hyaluronic acid, without the use of any chemical initiator. Dex-ox forms a hydrogel in the presence of gelatin by Schiff-base reaction and the chains of HA form a semi-IPN that can be used as injectable hydrogel. The hydrogel was loaded with two different anti-inflammatory drugs: naproxen, a nonsteroidal anti-inflammatory drug (NSAID) widely used to inhibit inflammation and cartilage damage in osteoarthritis [23] or dexamethasone, an anti-inflammatory corticosteroid used by intra-articular injection for the treatment of osteoarthritis [24].

2. Experimental section

2.1. Materials

Phosphate saline buffered solution (PBS, pH 7.4, Sigma-Aldrich), sodium periodate (NaIO_4 , Alfa Aesar, USA), potassium dihydrogen phosphate ($\text{KH}_2\text{PO}_4 \cdot 2\text{H}_2\text{O}$, Merck, Fluka), sodium phosphate dibasic ($\text{Na}_2\text{HPO}_4 \cdot 2\text{H}_2\text{O}$, Sigma-Aldrich, Germany), hydroxylamine hydrochloride (Sigma-Aldrich) and dextran with a M_w of 70 kDa (Dex70, Pharmacosmos, Denmark) were purchased and used without further purification.

High molecular weight hyaluronic acid (HA) with a M_w of 800-1000 kDa and free of endotoxins was kindly supplied by Bioiberica S.A. (Barcelona, Spain) and used as received.

Phosphate buffer pH 7.4 and 0.025M (PB) was prepared by dissolving the appropriate amounts of $\text{Na}_2\text{HPO}_4 \cdot 2\text{H}_2\text{O}$ and $\text{KH}_2\text{PO}_4 \cdot 2\text{H}_2\text{O}$ in deionized water and by adjusting the pH using HCl or NaOH.

2.2. Preparation and characterization of oxidized dextran (Dex70-ox)

Dex70 (3 g) was dissolved in distilled water (100 mg/mL). NaIO_4 solution (12 mL, 100 mg/mL) in distilled water were added drop by drop to the dextran solution. The mixture was protected from light and stirred for 4 hours, when an equimolar amount of ethylene glycol was added to stop the oxidation reaction. The resultant solution was purified by dialysis against distilled water (molecular weight cut-off = 1000) for 3-5 days. After dialysis, the solution was lyophilized and the oxidized dextran (Dex70-ox) characterized.

Oxidation degree determination: Oxidation degree of Dex70-ox was determined by the hydroxylamine hydrochloride titration method described by Zhao *et al.* [25] In this method, an excess of hydroxylamine hydrochloride reacted with Dex70-ox generating hydrochloric acid. The amount of hydrochloric acid produced is directly related with the aldehyde content in Dex70-ox and can be determined by simple titration with NaOH according to the equation (1):

$$\text{Oxidation degree (\%)} = \frac{V_{\text{NaOH}} \times N_{\text{NaOH}}}{W_{\text{sample}} \times M_{\text{W Dex}}} \quad \text{Equation (1)}$$

Where V_{NaOH} is the consumed volume of NaOH in the titration process, N_{NaOH} is the concentration of NaOH solution (0.1M), W_{sample} is the dry weight of Dex70-ox and M_{WDex} is the molecular weight of the repeating unit of Dex70.

Nuclear Magnetic Resonance (NMR): ^1H and ^{13}C Nuclear Magnetic Resonance (NMR) spectra were recorded on a Bruker Avance 400 spectrometer (Bruker Optik GmbH, Germany), operating at frequencies of 400 and 100 MHz, respectively, using deuterium oxide (D_2O) as solvent.

Molecular weight distribution: Molecular weight distribution was analyzed by Gel Permeation Chromatography (GPC) using a GPC equipment (Shimadzu 20A, Japan) equipped with a set of chromatography columns PL Aquagel-OH with different cut offs (Agilent, USA). Water was used as mobile phase at 1 mL/min and the GPC columns were heated at 40 °C. The apparent molecular weight obtained was determined by comparison with a calibration curve obtained with Pullulan® references (180 – 708000 Da, Varian, USA).

2.3. Design and characterization of an injectable hydrogel-based drug delivery system (IHDDS)

To quickly determine the time needed to form the gel, Dex70-ox and HA were dissolved in phosphate buffer (PB) and mixed at different ratios with a gelatin solution in PB at 37 °C. Briefly, the solutions were mixed and allowed to crosslink. The best crosslinking time (around 20 minutes) was determined by the inversion vial method and observation of the gel formation. The composition of this sample was used in this work and constituted the injectable hydrogel (IH).

The IHDDS was designed in a two components (A and B) ready to mix system that allows mixing and manipulation before injection. In this case, the hydrogel was loaded with two different anti-inflammatory drugs (12 mg/mL), naproxen or dexamethasone in different formulations (Table 1).

Table 1: Final composition of the different IHDDS prepared

Component A V= 0.5 mL	Component B V= 0.5 mL
--------------------------	--------------------------

Name	Gelatin [mg/mL]	Naproxen [mg/mL]	Dexamethasone [mg/mL]	Hyaluronic Acid [mg/mL]	Dex70-Ox [mg/mL]
IH	100	-	-	40	100
IHDDS-Nap	100	12	-	40	100
IHDDS-Dex	100	-	12	40	100

2.4. Hydration / degradation studies

IH, IHDDS-Nap and IHDDS-Dex formulations were prepared and let them to form the corresponding gel which was dried with filter paper to remove the exuded water. Each hydrogel was weighed (W_h) and subsequently introduced in 10 mL of PBS of pH 7.4 and transferred to an incubator at 37 °C. At different intervals of time, each sample was taken out of the medium and accurately weighed after removing rests of external water. Then, the hydrogel was introduced again in the same medium until the next time interval. The hydration/degradation ratio (H/D) was determined using the equation (2):

$$H/D = (W_t - W_h)/W_h \quad \text{Equation (2)}$$

Where W_t is the weight of the hydrated sample at time t. A minimum of three replicates were measured for each simple and values were given as average \pm standard deviation (SD).

2.5. Anti-inflammatory release experiments

The samples IHDDS-Nap and IHDDS-Dex were prepared as described in hydration/degradation studies subsection. The corresponding hydrogel sample was put in 10 mL of PBS of pH 7.4 at 37 °C. At different times, the medium was removed and replaced by fresh medium. The extracted medium was analyzed by UV spectroscopy using a NanoDrop one (Thermo Fisher Scientific) equipment analyzing the peak at $\lambda = 230$ nm for naproxen and at 243 nm for dexamethasone, and using calibration curves of known concentrations of NSAID and corticoid respectively. A minimum of three replicates were measured for each sample and values were given as average \pm SD.

2.6. Cell culture and *in vitro* tests

Three different cell lines were used in this work. Primary human osteoblasts (HOB, Innoprot) were grown and maintained in a mixture of Dulbecco's Modified Eagle Medium (DMEM, Sigma) and HAM-F12 (Sigma) supplemented with 10% of fetal bovine serum (FBS, Life Technologies) and 1% penicillin/streptomycin. Human articular chondrocytes (HAC, Innoprot) were grown in basal medium for chondrocytes (Innoprot) supplemented with 5% of FBS, 1% of chondrocyte growth supplement (Innoprot) and 100 units/mL penicillin/streptomycin. Human dermal fibroblasts (HDF, Innoprot) were cultured in DMEM supplemented with 10% FBS, 200 mM L-glutamine and 100 units/mL penicillin/streptomycin.

In all cases, the cells were incubated at 37 °C in a humidified atmosphere of 5% CO₂ and the cell culture media was refreshed every 3 days. Cells were used from 5-6 passages.

In vitro toxicity studies: In order to calculate the half-maximal inhibitory concentration (IC₅₀), a stock solution of Dex70-ox was prepared (80 mg/mL) in culture medium and consecutive dilutions were made. All solutions were sterilized by filtration using 20-micron filters.

For the toxicity of the IHDDS, the materials IH, IHDDS-Nap and IHDDS-Dex (prepared under sterile conditions) and the discs of the negative control Thermanox® (TMX, Labcrinics SL) were immersed in 5 mL of fresh and sterile medium and kept under stirring at 37 °C. After 1, 2, 7, 14 and 21 days, the medium was removed (leachates) and replaced with fresh medium.

In parallel, the cells (fibroblasts for Dex70-ox test and, chondrocytes and osteoblasts for IHDDS tests) were seeded, using fresh complete culture medium, at a concentration of $11 \cdot 10^4$ cells/mL, on 96-well plates. After adding 100 µL of cell concentrate in each well

and maintaining for 24 hours at 37 °C and an atmosphere with 5% CO₂, the culture medium was exchanged for the corresponding dilution or leachate (n = 8), and the plates were incubated for 24 hours under the same conditions. After this time, the contents of the wells were replaced by the MTT solution (10% in fresh medium). The MTT reagent was kept in contact with the cultures for 4 hours at 37 °C, and then, the content of the wells was extracted and 100 µL of dimethylsulfoxide (DMSO) was added, in order to dissolve the formazan crystals that may have formed. After a high intensity 20 s stirring, the optical density was read at 570 nm with a reference wavelength of 630 nm in a Biotek Synergy HT plate reader. The relative cell viability (% CV) was calculated with respect to the control, from the equation (3):

$$\% CV = \frac{OD_S - OD_B}{OD_C} \times 100 \quad \text{Equation (3)}$$

where OD_S, OD_B and OD_C are the optical density measurements of the sample, the blank and the control, respectively. Next, a dose-response curve of the relative cell viability vs concentration was plotted and the IC₅₀, defined as the concentration at which the death of 50% of the cells in the negative control occurs, calculated.

Cell viability assay: The cell viability of the hydrogels was measured by an Alamar Blue assay. The different IHDDS systems were directly deposited on a 24-well plate and let to form the gel for 30 minutes. Cells were seeded on the gels at a concentration of 14·10⁴ cells/mL in fresh complete culture medium

After the established time intervals (2, 7 and 14 days), the medium was removed from the wells and 1 mL of a 10% solution of Alamar Blue (Serotec, BUF012A) was added in complete medium without phenol red and incubated for 4 hours. The Alamar Blue was then replaced with fresh medium, transferred to a 96-well plate and measured the fluorescence at 570/630 (em/ex) in a microplate reader (Biotek Synergy HT spectrophotometer).

Statistical Analysis: Experimental data were expressed as the mean \pm SD (number of samples expressed in each figure). Statistical analyses were performed using one- way ANOVA followed by post- hoc Tukey honestly significant difference test with three levels of statistical significance: * $p < 0.05$, ** $p < 0.005$, *** $p < 0.001$

2.7. Design of an experimental model of osteoarthritis

Male New Zealand white rabbits (n=8) with an average body weight of 3860 g and 10 month old were used for the experimental studies. Animals were housed individually and had free access to tap water and pellet food in a temperature-controlled room with a 12 hours artificial day/night cycle. The animal experiments were carried out according to the European Directive (2010/63/EU) and the national Spanish law (RD 53/2013). Besides, the Ethical Committee of University of Salamanca approved surgical protocols (register number: 035). All animals were acclimatized for at least 2 weeks prior surgery. For the experimental model of osteoarthritis, collagenase type II (*Clostridium histolyticum* type II, activate enzyme 425 U/mg, Sigma-Aldrich) was dissolved in PBS at a concentration of 4 mg/mL and the solution was filtrated with a 0.22 μ m membrane. Animals were pre-anesthetized with an intramuscular injection of midazolam (5mg/ml) (Midazolam Normon) followed by general anesthesia by inhalation of 1.5% isoflurane (Forane®). After shaving with an electric shaver and sterilizing with 2% alcoholic chlorhexidine (Bactiseptic Orange) the knee joint was injected intra-articularly following the timeline proposed by Kikuchi *et al.* [26]

- Control group (n=6): two injections of PBS at 0 and 3 days.
- Osteoarthritis group (n=2): three collagenase injections at 0, 3 and 21 days

Animals of control group were euthanized by lethal injection of sodium pentobarbital (120 mg/kg, Dolethal®) after 3 weeks. OA group was used to evaluate the degree of osteoarthritis evoked and animals were sacrificed after 4 weeks.

2.8. Treatment of the osteoarthritis process with IHDDS

Three different treatments were applied on previously described osteoarthritis model which were divided in three groups, considering the initial experimentation time as the time of the first collagenase injection: :

- OA evolution group (n=2): two injections (0.3 mL) of PBS at 4 and 6 weeks of experimentation time.
- IHDDS-Nap group (n=2): two injections (0.6 mL) of naproxen loaded hydrogel at 4 and 6 weeks of experimentation time.
- IHDDS-Dex group (n=2): two injections (0.6m L) of dexamethasone loaded hydrogel at 4 and 6 weeks of experimentation time.

Before infiltration, both hydrogel components were mixed and heated at 37 °C for 25 min. After this time, the studied hydrogels were injected intra-articularly. During the immediate postoperative period, all animals were kept under electric blanket, to prevent hypothermia. Control and observation of pain was treated with subcutaneous injection of tramadol (50 mg/ml, 12h Adolonta, Grünenthal Pharma) and antibiotic therapy of enrofloxacin (Ganadexil Enrofloxacin 5%, Invesa). All animals were euthanized at 8 weeks of experimentation time.

Macroscopic study of the osteoarthritis process: A visual analysis was made to follow the degree of osteoarthritis obtained after infiltration with collagenase. Likewise, the repair of osteochondral lesions at a macroscopic level was studied following the Yosioka scale [27] that assesses the state of the articular surface at a morphological

level, as is shown in **Table 2**. The images were obtained with a Sony digital camera (model DSCW800B).

Table 2. *Yosioka scale of osteoarthritis: macroscopic evaluation of articular cartilage.*

Grade	Description
1	Articular surface intact
2	Minimal fibrillation
3	Evident fibrillation
4	Erosion with exposed subchondral bone

In addition, the osteoarthritis grade was assessed following a modification of the histological scale described by Wakitani S. *et al.* adapted for our study [28]. The images were analyzed and evaluated according to 5 parameters (see Table 3). By adding up the score given to each parameter, we obtained the histological score for each subject individually, which represents the sum of all evaluated parameters, with the maximum potential value being 14.

Table 3: *Histological grading scale for cartilage degeneration*

Category	
Cartilage morphology	
Hyaline cartilage	0
Mostly hyaline cartilage	1
Mostly fibrocartilage	2
Mostly non-cartilage	3
Non-cartilage only	4
Cell morphology	
Intact, appropriate orientation	0
Proliferation (clusters), hypertrophy, superficial zone	1
Proliferation (clusters), hypertrophy, mid zone	2
Matrix-staining (safranin-O)	
Normal (compared with control group: normal cartilage)	0
Slightly reduced	1
Marked reduced	2
No stain	3
Surface regularity	

No discontinuity	0
Irregularities at the superficial zone	1
Progression into mid zone	2
Progression into deep zone	3
<hr/>	
Thickness of cartilage	
>2/3	0
1/3-2/3	1
<1/3	2
<hr/>	
Total maximum	14

Histological study: Once rabbits were sacrificed at each experimentation time, the knees joints were resected. The distal metaphysis of the femur was dissected and sawed sagittally at the level of the medial condyle. Bone samples were fixed in 4% paraformaldehyde and decalcified in DC3 reactive (VWR Chemicals Prolabo®, France) during 48 hours. After decalcification, bone samples were embedded in paraffin. Five micrometer-thin sections were stained with Hematoxylin and Eosin (H/E) to study cellular cartilage components and with Safranin-O/Fast green (S-O) to detect proteoglycan loss in cartilage by light microscopic examination.

Immunohistochemical technique for detection of type II collagen: Paraffin sections were deparaffinized and incubated in 10 mM citrate-based buffered solution (pH 6.0) during 1 min for antigen unmasking (Vector Laboratories, Inc., USA). Immunostaining was performed using a mouse monoclonal collagen type II antibody (mouse mAb II.4C11, Calbiochem, USA), dilution of 1:100 overnight and revealed with the Vectastain® ABC Kit (Vector Laboratories, Inc., USA) following manufacturer instructions. Immunostained sections were counterstained with Hematoxylin.

Stained sections were evaluated and photographed by a bright field microscope (Nikon Eclipse 90i) equipped with a Nikon Digital Sight DS-smc camera (Nikon Corporation, Japan).

3. Results and discussion

3.1. Design and characterization of an injectable hydrogel-based drug delivery system (IHDDS)

Partially oxidized dextran with a molecular weight (M_w) of 70 kDa (Dex70-ox) was first prepared using sodium periodate (NaIO_4) as oxidant. To quantify the aldehyde groups in Dex70-ox, the hydroxylamine hydrochloride titration method was used, getting a 40 % of oxidation degree. $^1\text{H-NMR}$ spectrum corroborates the formation of aldehyde groups by the new peaks appeared between 3.9 ppm and 6.0 ppm that correspond with the hemiacetal formation in Dex70-ox [29] (Figure S1 in supplementary data).

The degradation of Dex70-ox and its stability with the time in phosphate saline buffered solution (PBS) at 37°C were evaluated by GPC (Figure 1).

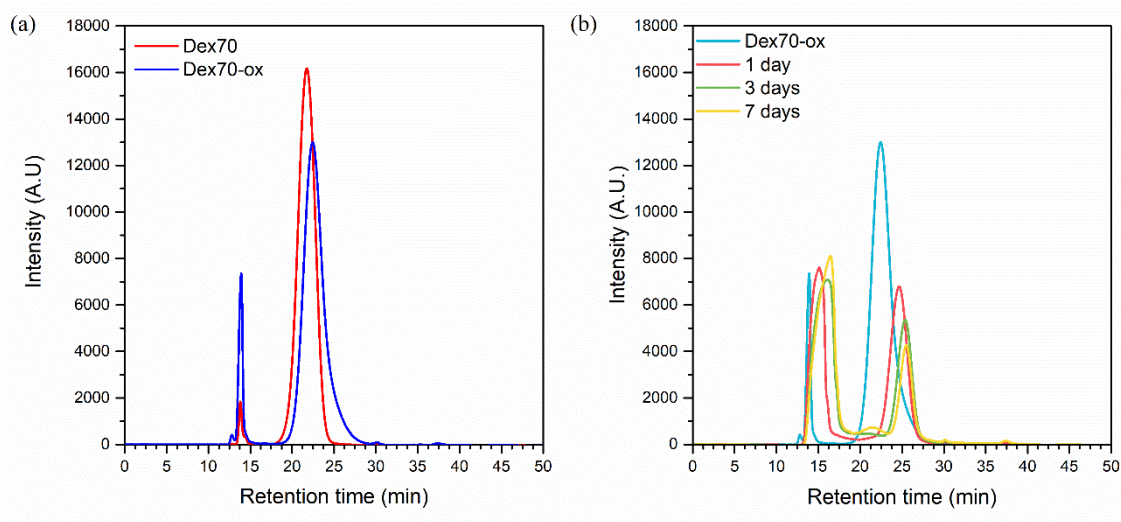


Figure 1: Results of the GPC analysis comparing Dex70 and Dex70-ox (a) and the hydrolysis of Dex70-ox with time in PBS at 37°C (b).

After oxidation (Figure 1a), the molecular weight obtained from the principal signal in the chromatogram of Dex70 decreases from a $M_w = 62$ kDa to 40 kDa due to the

periodate oxidation, but it also appears a new signal at lower retention time with a molecular weight (around 250 kDa). Maia *et al.* described this behavior due to that the oxidation process favors the inter-chain hemiacetals formation, resembling a molecular weight increasing [29].

The hydrolysis of Dex70-ox (Figure 1b) decreases the principal M_w , but increases the number of low molecular weight species, attributed to a rise in the interactions between hemiacetals groups. For this reason, there is an increase in the relation between high molecular weight species/low molecular weight species [29]. The study of the NMR of the Dex70-ox incubated at different times showed that there is not changes in the chemical structure (Figure S2 in supplementary data), therefore the hydrolysis only affects the molecular weight.

The injectable hydrogel (IH) was designed as two components ready to use system (Table 1 in Experimental Section and Figure S3 in supplementary data) loaded with naproxen (IHDDS-Nap) or dexamethasone (IHDDS-Dex). Hydrogels were prepared by mixing equal volumes of PBS solutions containing gelatin and the anti-inflammatory drug (Component A) with hyaluronic acid and Dex70-ox (Component B). The crosslinking reaction is due to Schiff's base formation between the amino groups of the gelatin and the aldehyde groups of Dex70-ox trapping the hyaluronic acid among the crosslinked gelatin and forming a semi-interpenetrated network (semi-IPN). The gelation process takes around 20 minutes.

3.2. Hydration/degradation behavior (H/D) and in vitro anti-inflammatory release experiments

The administration of NSAID [30] and corticoids [31] into the synovial cavity is performed in clinical practice to treat OA but this route involves several drawbacks [32]. Therefore, the in situ administration of the drug embedded in a hydrogel structure

[33, 34] is expected to provide some benefits such as reduce the low *in situ* retention time. Consequently, research on this topic is nowadays increasing [32, 35]. In this sense, recently Feng *et al.* developed cell-infiltratable and injectable gelatin hydrogels physically and chemically crosslinked that can mediate release of small hydrophobic drugs such as icaritin to promote differentiation of stem cells [36]. Zhang *et al.* developed injectable bioactive nanocomposites based on hyaluronic acid and pamidronate-magnesium nanoparticles for the release of dexamethasone to stimulate bone regeneration [37]. In this context, the IHDDS hydrogels loaded with naproxen or dexamethasone can be considered as a novel approach in the treatment of OA. To investigate the *in vivo* fate of the developed cargo systems, swelling, degradation and drug release behavior were first analyzed.

The swelling capacity of the hydrogels is an indication of the degree of hydrophilicity [38] and influences cellular behavior [39]. In this work, the stability of the hydrogels was analyzed *in vitro* by soaking the samples in PBS (pH of 7.4) at 37 °C up to 15 days. Results of the hydration /degradation ratio are displayed in Figure 2a. In the first 180 min an increase in the H/D ratio occurs indicating that hydration prevails over degradation as a consequence of the water absorption. At this point (180 min) the maximum H/D value for the nude hydrogel (IH) is 1.2 whereas is 1.1 for those charged with drugs. Next, the H/D ratio decreases because of the degradation phenomenon and the release of the drug. The fastest H/D decrease is for the IHDDS-Nap sample which completely degrades within 16 days, followed by the IH sample that totally disintegrates after 24 days. The IHDDS-Dex sample degrades progressively and maintains its integrity even up to 30 days (data not shown)

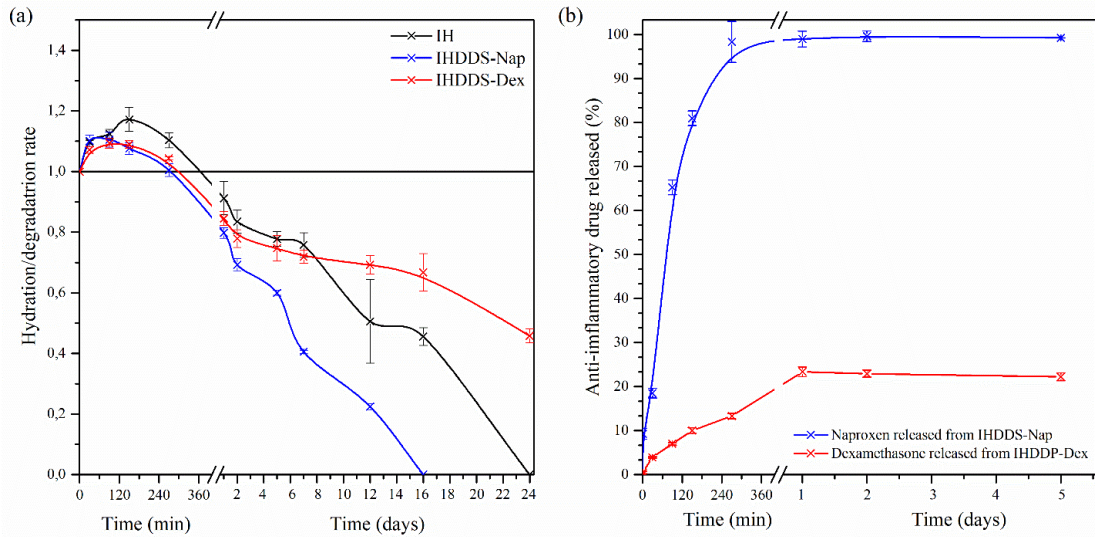


Figure 2 (a). Variation of hydration/degradation with immersion time of the different hydrogels soaked in PBS of pH 7.4 at 37 °C ($n=3$). **(b)** Release profiles of naproxen and dexamethasone from the IHDDS-Nap and IHDDS-Dex hydrogels respectively, in PBS of pH=7.4 at 37 °C ($n=3$).

Similar results are reported in literature. Kurisawa *et al.*, found that the degradation of gelatin and dextran IPN hydrogels occurs approximately in the first 24 h [40] and in relation to hydrogels loaded with corticoid, Fan *et al.* observed a degradation of a HA and furan hydrogel charged with dexamethasone in a period of 21 days [41]. In our study, the stability of the hydrogels loaded with naproxen or dexamethasone is good for 2 and, at least 4 weeks, respectively. Particularly, the hydrogels loaded with dexamethasone are much more stable and, taking into consideration the application in regeneration of cartilage defects, these hydrogels seem to be much more appropriate. Even, it is very likely that they are stable for longer times, considering that at one-month period, the samples still maintain good dimensional stability.

Drug release and degradation are two phenomena that take place simultaneously and therefore, their corresponding mechanisms are inter-related. On the one hand, degradation of hydrogels crosslinked via Schiff-based reaction can occur due to the

dynamic nature of these linkages [42] [43], and on the other hand, release mechanism of entrapped drugs is mediated via diffusion in which solubility of the drug plays a crucial role. Moreover, in the semi-IPN systems the release of HA over time will also contribute to degradation of the system. Release profiles of the anti-inflammatory drugs in PBS of pH 7.4 at 37 °C is shown in Figure 2b. For the IHDDS-Nap hydrogels nearly the initial total content of naproxen is released in the first 240 min. These results correlate with those published by Peng *et al.*, who studied the release of naproxen from chitosan hydrogels with carbon nanotubes, and observed a release of more than 50% of the drug in the first 30 min [44].

However, the release profile for the IHDDS-Dex hydrogels is sustained from the beginning, and a content of 22 % of initial drug is released in five days. Accordingly, for a dexamethasone HA hydrogel, Fan *et al.*, reported a release of 26% of the dexamethasone loaded in 24 h reaching a plateau [41].

In our systems the very different degradation and drug release behavior between the naproxen and dexamethasone loaded systems may be ascribed to the different hydrophilic/hydrophobic character of the drugs and hence, to their different solubility, but also to the different interactions of the drugs with the polysaccharides via hydrogen bonds. Naproxen presents higher solubility in PBS than dexamethasone due to the carboxylic acid in its structure, whereas the more hydrophobic dexamethasone is more prone to interact through hydrogen bonds with dextran and hyaluronic acid due to the three hydroxyl groups of its structure. Moreover, hydrogen interactions among dexamethasone/HA/dextran/gelatin can reinforced the higher integrity of this hydrogel. This approach opens a window of IHDDS that can be formulated by changing composition of the semi-IPN and/or the drug, tuning the degradation and release profile of the system for each specific case.

3.3. *In vitro* cytotoxicity analysis

The toxicity of components A and B of the IH can be derived from that of Dex70-ox due to the presence of aldehyde groups. Therefore, the cytotoxicity of Dex70-ox was tested in the first place (Figure S4 in supplementary data). Dex70-ox presents a half maximal inhibitory concentration (IC_{50}) of 20 mg/mL. Taken into account that the residual concentration of aldehyde groups will decrease markedly after the crosslinking reaction with gelatin it is expected that the biocompatibility of the injectable hydrogels, once the semi-interpenetrated network is formed, will not be compromised.

The toxicity of the IH and IHDDS was tested in chondrocytes and osteoblasts cultures, using the leachates of hydrogels taken at different periods after the immersion of the hydrogels in culture medium. (Figure 3).

IH and IHDDS present a significant decrease in cell viability (CV) on chondrocytes due to the release of unreacted Dex70-ox and the release of the drugs; nonetheless, the cell viability is always higher than 80% and is partially recovered with the time. In the case of osteoblasts, a significant effect on cell viability is only observed in IHDDS samples, mainly due to the release of the drugs. In the IHDDS-Nap sample there is a significant decrease only in the first 24 hours due to the fast release of naproxen, but cell viability recovers with the time. Instead, as IHDDS-Dex sample presents a slower release of dexamethasone, the decrease of cell viability is evident at longer times (7 and 14 days) but it recovers at 21 days.

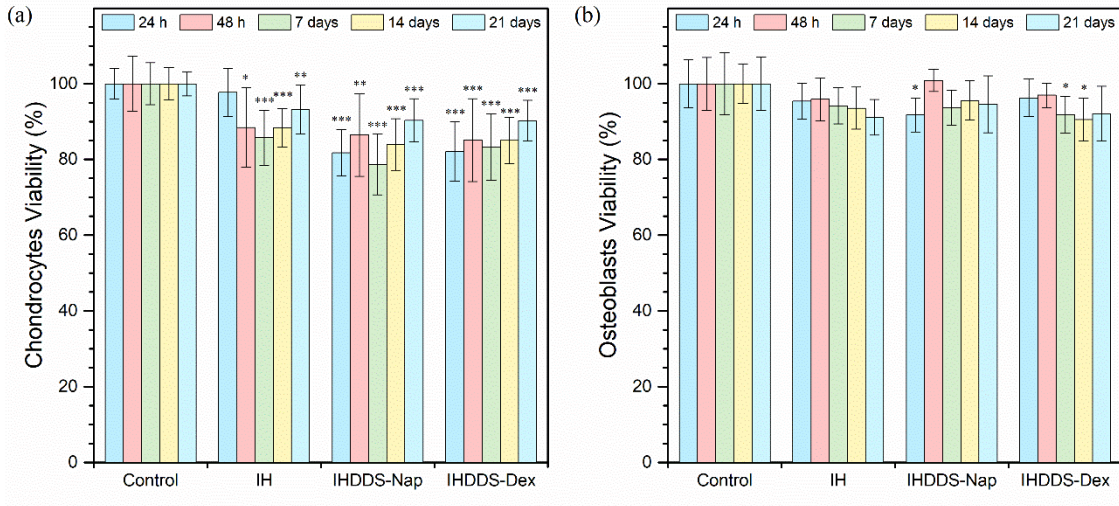


Figure 3. Cytotoxicity of the leachates of the different systems on chondrocytes (a) and osteoblasts (b) compared with the TMX control ($n = 4$, * $p < 0.05$, ** $p < 0.005$, *** $p < 0.001$)

3.4. In vitro cell viability studies

Alamar Blue assay was used to study the cell viability of chondrocytes and osteoblasts directly seeded on the different IHDDS. The hydrogel without drug (IH) was used as control and the cell viability results were normalized with it. The results are shown in Figure 4:

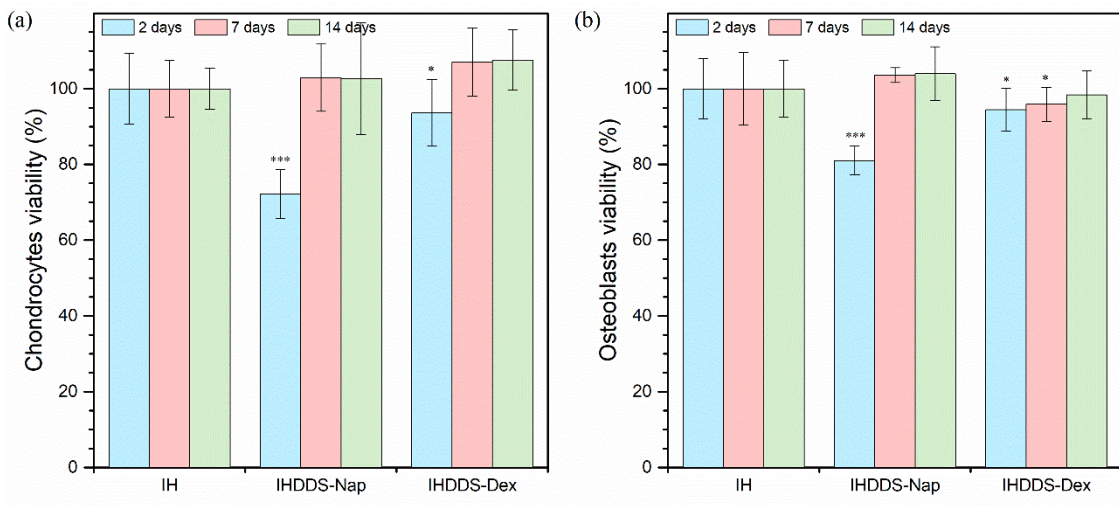


Figure 4. Cell viability of the different systems using chondrocytes (a) and osteoblasts (b) compared with the behavior in the IH ($n = 6$, * $p < 0.05$, ** $p < 0.005$, *** $p < 0.001$)

Wu *et al* claim that hyaluronic acid hydrogels are not cytotoxic and stimulate cell proliferation [45]. In our case, chondrocytes and osteoblasts viability is high in presence of both IHDDS at long times (14 days) .IHDDS-Nap shows a significant decrease in cell viability in the first 2 days due to the rapid release of naproxen. After 7 days the viability in both cell lines is comparable to the IH, the CV being slightly higher for chondrocytes. Summarizing, the *in vitro* results indicate that the developed injectable systems are not cytotoxic and support good cell viability in chondrocytes and osteoblasts cultures; hence, they can be adequate candidates to be used in the osteoarthritis process.

3.5. *In vivo* macroscopic study of the osteoarthritis process treated with IHDDS

The efficacy of the IHDDS systems was tested *in vivo* by intra-articular injection in New Zealand rabbits using an osteoarthritis (OA) model. The evolution of the osteoarthritis was studied macroscopically. The control knee (three injections of PBS) (Figure 5a) presents a normal external appearance without macroscopic change of the articular cartilage. On the other hand, the OA group (three injections of collagenase) (Figure 5b) presented greater joint swelling, hematoma and, inflamed and hyperemic synovial membrane (Figure 5b.1 and 5b.2). Considering the scale of Yosioka [27] in the macroscopic study of articular cartilage, the OA group presented hemarthrosis and minimal joint fibrillation in the internal femoral condyle without exposing the subchondral bone (Grade 2-3 of Yosioka scale (Table 3). Figure 5b.3, indicated with *).

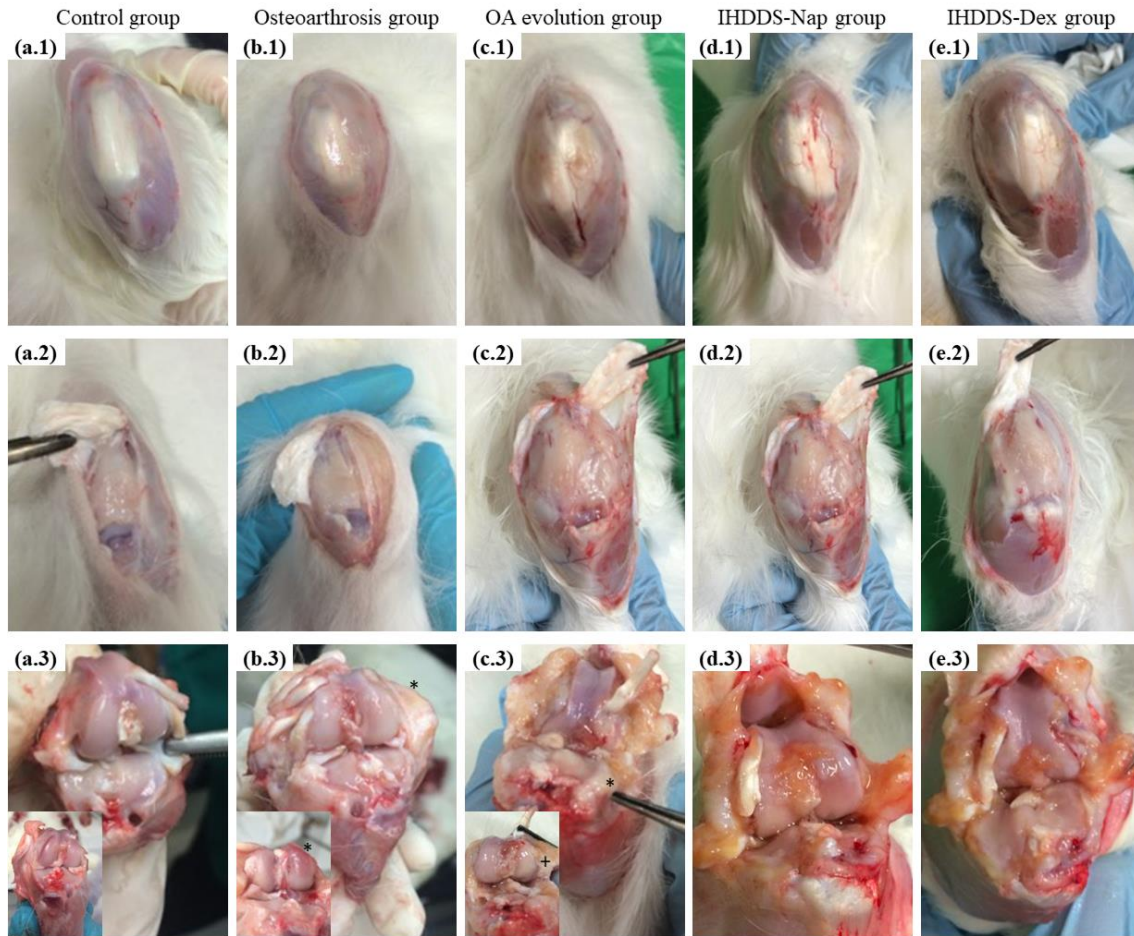


Figure 5. Macroscopic study of the osteoarthritis evolution. (a) Control group, (b) OA group, (c) OA evolution group, (d) IHDDS-Nap group and (e) IHDDS-Dex group. (1) Macroscopic view of the joint capsule. (2) Macroscopic view of the synovial membrane. (3) Macroscopic view of the articular cartilage

The evolution of the osteoarthritis without treatment (OA evolution group. Figure 5c) presents more severe degenerative changes. The knee presents a greater hypertrophy of the joint capsule (Figure 5c.1) with the synovial membrane more congestive, inflamed and thickened (Figure 5c.2). The articular cartilage is affected with presence of osteophytes in the tibial plateau (* in Figure 5c.3) and the external femoral condyle presents an irregular appearance with a clear exposure of subchondral bone (+ in Figure 5c.3). These results are similar to those obtained by Kikuchi *et al.* [26] and can be evaluated as Grade 3 of Yosioka scale.

The treated knees with naproxen loaded hydrogel (IHDDS-Nap group) present capsular hypertrophy with a lower proportion of hemarthrosis and lower degree of fibrosis in the soft tissues (Figure 5d.1 and 5d.2). The articular cartilage does not present osteophytes but a femoral chondral lesion without subchondral bone exposure can be observed (Grade 2 of Yosioka scale. Figure 5d.3). In the case of dexamethasone loaded hydrogels (IHDDS-Dex group), this group presents a higher level of fibrosis of the soft tissues (Figure 5e.1 and 5e.2) but not clear chondral injury can be observed in the joint (Figure 5e.3)

The knees treated with the IHDDS present a lower macroscopic degree of osteoarthritis with a better recovery in the case of IHDDS-Dex group.

In addition, the osteoarthritis grade was evaluated following a modification of the histological scale described by Wakitani S. *et al* [28]. Thus, the qualitative histological observations were scored according to the parameters included in Table 3, and the obtained values of cartilage degeneration were represented in Table 4. It can be seen that the cartilage treated with the anti-inflammatory drugs gave rise to the lower score grades, the one loaded with dexamethasone being the lowest which correlated with previous findings.

Table 4. Results of the histological grading scale

	Grade (points)					Total
	Cartilage morph.	Cell morph.	Matrix-staining	Surface regularity	Thickness of cartilage	
OA group	1.8	1.7	1.5	1.8	0.4	7.2
OA evolution	2.5	2	1.8	2.5	1.5	10.3

IHDDS-Nap	1.6	1.6	1.3	1.3	0.7	6.5
IHDDS-Dex	1.2	1.5	2	1	0.5	6.2

3.6. Histological study of the osteoarthritis process treated with IHDDS

Results of the histopathological studies are represented in Figure 6. H/E stained sections of the control group (Figure 6a.1 and a.2) revealed no histological changes in the articular cartilages. Articular surface was smooth and continuous. Normal hyaline cartilage is distinguished by the presence of homogeneous and amorphous ECM. No fissures were present. Cartilage showed normal architecture of chondrocytes, aligned in vertical rows, inside lacunae and forming isogenic groups. Subchondral bone presented a normal morphology and homogeneous vascularization.

In the case of OA group, microscopic images showed a degenerative cartilage (Figures 6b.1 and b.2). The articular surface was broken and cracked, with isolated fragments of cartilage detached from the articular surface. Notable and deep fissures were evident. The cellular disposition was disrupted, showing chondrocytes hypertrophy and hypercellularity. Nevertheless, subchondral bone appeared preserved with unaltered vascularization.

OA evolution group presented a remarkable cartilage degeneration (Figure 6c.1 and c.2). Notable surface irregularity was evident, where numerous fissures and erosions could be noticed. Deep fissures extended down to the deep zone reaching the tidemark. The thickness of the articular cartilage layer was greatly reduced. Isolated detached cartilage fragments were also observed. Chondrocytes density was decreased and morphologically changed, being hypertrophic, disorganized and forming clusters in order to adjust to the changing microenvironments [46]. Subchondral bone showed altered and irregular tidemark disposition with several calcification fronts. Tidemark changes were characterized by duplication and penetration, where tidemark suffered

multiple episodes of advancement and appeared breached due to vascular invasion, losing its integrity. This tidemark changes were classified into different degrees of severity in an osteoarthrosis model [47]. Tidemark breaching was recognized in end-stage OA in both animal [48] and human models [49]. Furthermore, subchondral bone presented a higher vascularization degree. These processes are related to tidemark multiplication and vascular invasion in human OA [50].

In the IHDDS-Nap group a relative cartilage repair response could be seen (Figure 6d.1 and d.2). Articular surface showed little fragmentation and fissures were shallow. The thickness of the articular cartilage layer was similar to the normal cartilage. Both extracellular matrix and chondrocytes showed a preserved structure, although hypocellularity was observed. Chondrocytes parallel disposition and forming columns reminded normal articular cartilage. Isolated hypertrophic chondrocyte clusters were present but never at the superficial zone. Duplication and vascular penetration of the tidemark could be seen.

Finally, IHDDS-Dex group, as the previous group, presented a relative conserved articular cartilage (Figure 6e.1 and e.2). Increased thickness of the cartilage regeneration occurred. Surface zone was partly smooth with little and shallow fissures. Scarce detached cartilage fragments were observed. Extracellular matrix showed a heterogeneous stain. Hypertrophic chondrocytes forming clusters showed an augmented basophilic stain at the territorial matrix being more evident at superficial zone. Chondrocyte density was increased in comparison with IHDDS-Nap group, but no organization in columns occurred. Both tidemark and subchondral bone were preserved, and normal vascularization was appreciated.

In both IHDDS groups, articular cartilage was more preserved in comparison with OA groups. IHDDS-Nap group presented superficial fissures and mild surface

discontinuities, whereas IHDDS-Dex group showed surface undulation, without irregularities, being more conserved. In both groups, increased thickness of the cartilage regeneration occurred. Chondrocyte hypocellularity was more evident in IHDDS-Nap group. In addition, cellular distribution was different between hydrogels groups. In IHDDS-Nap group, linear chondron columns were aligned in parallel whereas in IHDDS-Dex group, chondron clusters, formed by numerous chondrocytes, were radially distributed. As previously said, proliferative chondrocytes form clusters in order to adjust to the changing microenvironments and to promote repair processes [46].

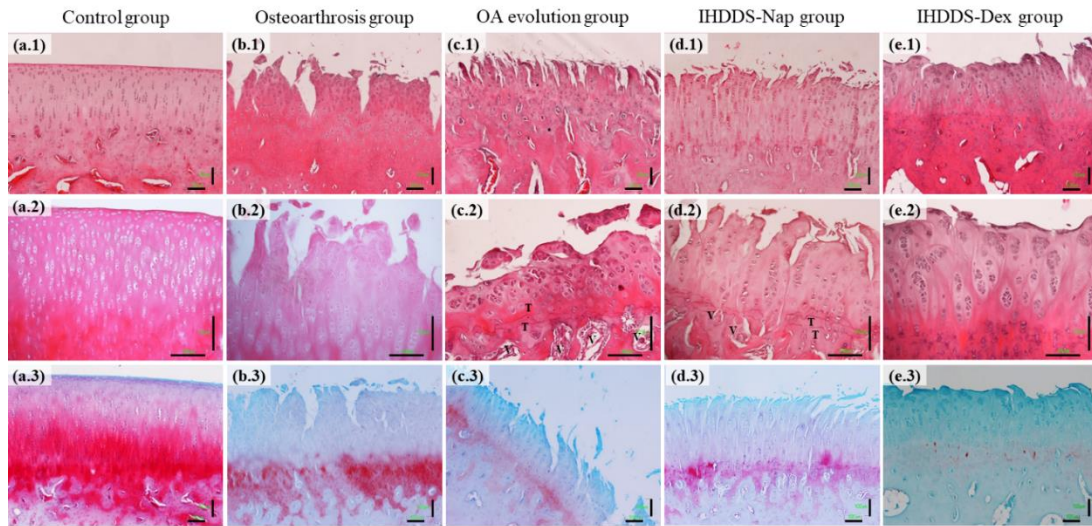


Figure 6. Hematoxylin/Eosin (1 and 2) and Safranin-O (3) stain micrographs of rabbit articular cartilage of studied groups: (a) control group, (b) OA group, (c) OA evolution group, (d) IHDDS-Nap group and (e) IHDDS-Dex group. Hematoxylin/Eosin stain at (1) 10x and (2) 20x. Scale bars: 100 μm . T: Tidemark. V: Vascularization. (3) Safranin-O stain, 10x, scale bars: 100 μm

The cartilage extracellular matrix composition could be determined through the Safranin-O (S-O) staining method. An absence or decrease in staining (red color) revealed the loss of proteoglycans, which was significantly reduced in the IHDDS-Dex group (Figure 6e.3 and S5) compared to the normal cartilage (Figure 6a.3). The other three groups: OA group (Figure 6b.3), OA evolution group (Figure 6c.3) and IHDDS-

Nap group (Figure 6d.3) showed a slightly reduced S-O stainability, not resulting in a marked loss of proteoglycans.

In particular, normal cartilage showed homogeneous S-O stain through the articular cartilage, representing the normal presence of proteoglycans at ECM in physiological conditions (Figure 6a.3). OA group manifested a loss of staining at the surface cartilage layer. The rest of cartilage extracellular matrix showed a weak stain, being more intense at the calcified zone (Figure 6b.3). OA evolution group showed a reduction of S-O stain down to the transitional layer. In comparison with previous group, the stain of calcified layer was reduced, sign of PG loss (Figure 6c.3). Proteoglycans loss at the upper-zone evoked an alteration in mechanical properties of articular cartilage at this level [51, 52]. The alteration of cellular configuration, such the evidence of proliferative chondrocytes forming clusters in OA evolution group, also changes the quantity and composition of the ECM secreted by the cells. The reduced proteoglycans content decreases compressive modulus of cartilage and consequently exposes the tissue to greater strains when exposed to mechanical stress [46, 53].

IHDDS-Nap group showed a homogeneous S-O stain through the entire ECM except at the surface layer. Compared with the control group, the stain is less intense (Figure 6d.3). Finally, IHDDS-Dex group showed a severe reduction of stain revealing loss of PG. Only a poor staining in the calcified layer could be observed (Figure 6e.3 and S5). Corticosteroids can function as inhibitors of proteoglycans synthesis, worsening cartilage lesions or even causing a degenerative lesion in healthy joint cartilage [54, 55]. In our study, we observed similar results in which IHDDS-Dex had a negative effect in relation to PG content, which was clearly reduced. However, in relation with preservation of superficial cartilage zone, in IHDDS-Dex group it was relative maintained. Nevertheless, Pelletier *et al.* [56, 57] in different studies in osteoarthritis

model in dogs, demonstrated that low doses of intra-articular corticosteroids could normalize the synthesis of proteoglycans and could significantly decrease the incidence and severity of osteophyte formation and cartilage lesions.

3.7. Immunohistochemical study of the osteoarthritis process treated with IHDDS

The immunohistochemical detection of type II collagen allows to assess the quality of the extracellular matrix synthesized by chondrocytes, assigning it characteristics of hyaline cartilage and distinguishing it from the fibrous tissue repair synthesized by the fibroblasts [58]. The immunostaining expression of collagen type II was represented in Figure 7. The positive immunostaining for collagen type II was intense throughout the totality of cartilage matrix in control group (Figure 7.a). In OA group, the immunoreactivity showed a marked reduction in almost the totality of the articular cartilage, being only the calcified layer positively immunostained (Figure 7.b). Accordingly, OA evolution group showed no collagen type II immunoreactivity (Figure 7.c). Regarding IHDDS-Nap group, the positive immunostain was weak at the interterritorial matrix, whereas it was moderate at the calcified zone (Figure 7.d). Finally, in IHDDS-Dex group the immunoreactivity was positive in the interterritorial areas, especially delimiting the chondrocytes clusters. Besides, the calcified layer was intensely immunostained (Figure 7.e).

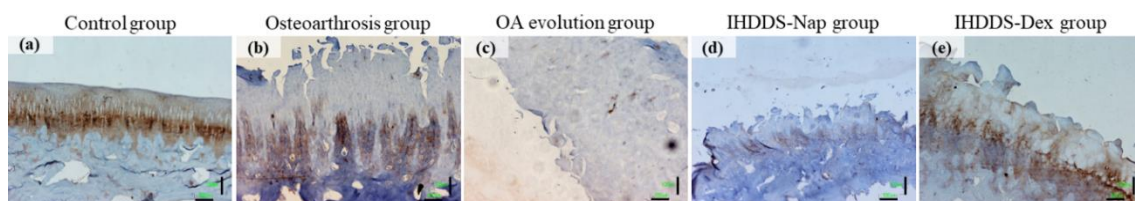


Figure 7. Anti-collagen II immunostaining micrographs of articular cartilage from rabbit femoral condyles. (a) Control group, (b) OA group, (c) OA evolution group, (d) IHDDS-Nap group and (e) IHDDS-Dex group. 10x, scale bars: 100 μm .

Especially, in the OA evolution group we have appreciated the articular cartilage degeneration development, altering ECM composition to the detriment of the presence of collagen type II. This behavior was also appreciable in an established osteoarthritic model [59, 60].

However, immunoreactive collagen type II expression was significantly higher in IHDDS groups compared with OA evolution group. This increased collagen type II expression reflects an ECM recovery from the damaged cartilage, being more evident in IHDDS-Dex group especially at the matrix surrounding chondron. Also, the increase of collagen type II indicates a regenerative effort by chondrocytes to compensate the collagen type II lost. The use of dexamethasone decreases the inflammatory reaction and the production of metalloproteinases resulting in an increase expression of type II collagen [61, 62].

4. Summary and Conclusions

In this work, injectable hydrogels loaded with an anti-inflammatory drug, naproxen (IHDDS-Nap) or dexamethasone (IHDDS-Dex) have been developed based on a simple two components system. The drug release profile strongly depended on the degradation pattern which differed for each IHDDS. The injection of the loaded hydrogels in New Zealand rabbits knees after created an osteoarthrosis (OA) indicate that IHDDS presented low macroscopic degree of OA, with a better recovery for the IHDDS-Dex group. The histological analysis revealed preservation of the cartilage in both drug loaded systems and collagen type II expression in the ECM, more evident for the IHDDS-Dex group. These promising results suggest that the IHDDS can be considered an alternative to currently used treatments in OA and should be analyzed in further studies.

Supporting Information

Supporting Information is available from the Wiley Online Library or from the author.

Acknowledgements

This work was supported by the Ministry of Science, Innovation and Universities (Spain) (MAT2017-2017-84277-R) and CIBER-BBN (Instituto de Salud Carlos III, Spain).

The authors thank Rosana Ramirez (ICTP-CSIC) for the excellent technical assistance with cell culture experiments and the Department of Human Anatomy and Histology of Faculty of Medicine, University of Salamanca, for assistance in histological preparations.

References

- [1] R. Barbucci, S. Lamponi, A. Borzacchiello, L. Ambrosio, M. Fini, P. Torricelli, R. Giardino, *Biomaterials*, 23 (2002) 4503-4513.
- [2] Z. He, B. Wang, C. Hu, J. Zhao, *Colloids Surf. B. Biointerfaces*, 154 (2017) 33-39.
- [3] A.D. Sánchez-Téllez, L. Téllez-Jurado, M.L. Rodríguez-Lorenzo, *Polymers*, 9 (2017).
- [4] J.M. Case, J.M. Scopp, *Sports Med Arthrosc Rev*, 24 (2016) 63-68.
- [5] C. Erggelet, *Oper. Tech. Orthop.*, 24 (2014) 2-13.
- [6] T. Murakami, N. Sakai, T. Yamaguchi, S. Yarimitsu, K. Nakashima, Y. Sawae, A. Suzuki, *Tribology International*, 89 (2015) 19-26.
- [7] H. Tan, K.G. Marra, *Materials*, 3 (2010).
- [8] M.D. Brigham, A. Bick, E. Lo, A. Bendali, J.A. Burdick, A. Khademhosseini, *Tissue Engineering Part A*, 15 (2008) 1645-1653.
- [9] L. Pescosolido, W. Schuurman, J. Malda, P. Matricardi, F. Alhaique, T. Coviello, P.R. Van Weeren, W.J.A. Dhert, W.E. Hennink, T. Vermonden, *Biomacromolecules*, 12 (2011) 1831-1838.
- [10] X. Geng, L. Yuan, X. Mo, 2013, pp. 745-750.

- [11] Y. Huang, S. Onyeri, M. Siewe, A. Moshfeghian, S.V. Madihally, *Biomaterials*, 26 (2005) 7616-7627.
- [12] K.L. Goa, P. Benfield, *Drugs*, 47 (1994) 536-566.
- [13] J.R.E. Fraser, T.C. Laurent, U.B.G. Laurent, *J. Intern. Med.*, 242 (2003) 27-33.
- [14] J. Yang, Y.S. Zhang, K. Yue, A. Khademhosseini, *Acta Biomater.*, 57 (2017) 1-25.
- [15] A. Mora-Boza, M. Puertas-Bartolomé, B. Vázquez-Lasa, J. San Román, A. Pérez-Caballer, M. Olmeda-Lozano, *European Polymer Journal*, 95 (2017) 11-26.
- [16] H.-W. Sung, R.-N. Huang, L.H. Huang Lynn, C.-C. Tsai, C.-T. Chiu, *J. Biomed. Mater. Res.*, 42 (1998) 560-567.
- [17] Y.D. Park, N. Tirelli, J.A. Hubbell, *Biomaterials*, 24 (2003) 893-900.
- [18] H. Tan, C.R. Chu, K.A. Payne, K.G. Marra, *Biomaterials*, 30 (2009) 2499-2506.
- [19] J. Maia, L. Ferreira, R. Carvalho, M.A. Ramos, M.H. Gil, *Polymer*, 46 (2005) 9604-9614.
- [20] K.H. Lee, *The Quarterly Review of Biology*, 76 (2001) 228-229.
- [21] L. Weng, X. Chen, W. Chen, *Biomacromolecules*, 8 (2007) 1109-1115.
- [22] B. Hoffmann, D. Seitz, A. Mencke, A. Kokott, G. Ziegler, *J. Mater. Sci. Mater. Med.*, 20 (2009) 1495-1503.
- [23] A.J. Kivitz, R.W. Moskowitz, E. Woods, R.C. Hubbard, K.M. Verburg, J.B. Lefkowitz, G.S. Geis, *J. Int. Med. Res.*, 29 (2001) 467-479.
- [24] K.D. Huebner, N.G. Shrive, C.B. Frank, *J. Orthop. Res.*, 32 (2014) 566-572.
- [25] H. Zhao, N.D. Heindel, *Pharm. Res.*, 8 (1991) 400-402.
- [26] T. Kikuchi, T. Sakuta, T. Yamaguchi, *Osteoarthritis Cartilage*, 6 (1998) 177-186.
- [27] M. Yoshioka, R.D. Coutts, D. Amiel, S.A. Hacker, *Osteoarthritis Cartilage*, 4 (1996) 87-98.
- [28] S. Wakitani, T. Goto, S.J. Pineda, R.G. Young, J.M. Mansour, A.I. Caplan, V.M. Goldberg, *J. Bone Joint Surg. Am.*, 76 (1994) 579-592.
- [29] J. Maia, R.A. Carvalho, J.F.J. Coelho, P.N. Simões, M.H. Gil, *Polymer*, 52 (2011) 258-265.

- [30] M.M. Orak, D. Ak, A. Midi, B. Lacin, S. Purisa, G. Bulut, *Acta Orthop. Traumatol. Turc.*, 49 (2015) 438-446.
- [31] R. Klocke, K. Levasseur, G.D. Kitas, J.P. Smith, G. Hirsch, *Rheumatol. Int.*, 38 (2018) 455-459.
- [32] G.M. Pontes-Quero, L. Garcia-Fernandez, M.R. Aguilar, J. San Roman, J. Perez Cano, B. Vazquez-Lasa, *Semin. Arthritis Rheum.*, (2019).
- [33] T. Euppayo, V. Punyapornwithaya, S. Chomdej, S. Ongchai, K. Nganvongpanit, *BMC Musculoskelet. Disord.*, 18 (2017) 387-387.
- [34] F. Wang, X. He, *Exp. Ther. Med.*, 9 (2015) 493-500.
- [35] H. Zhou, C. Liang, Z. Wei, Y. Bai, S.B. Bhaduri, T.J. Webster, L. Bian, L. Yang, *Mater. Today*, (2019).
- [36] Q. Feng, J. Xu, K. Zhang, H. Yao, N. Zheng, L. Zheng, J. Wang, K. Wei, X. Xiao, L. Qin, *ACS central science*, 5 (2019) 440-450.
- [37] K. Zhang, Z. Jia, B. Yang, Q. Feng, X. Xu, W. Yuan, X. Li, X. Chen, L. Duan, D. Wang, *Advanced Science*, 5 (2018) 1800875.
- [38] J.W. Nichol, S.T. Koshy, H. Bae, C.M. Hwang, S. Yamanlar, A. Khademhosseini, *Biomaterials*, 31 (2010) 5536-5544.
- [39] J. Shi, M.M.Q. Xing, W. Zhong, *Membranes*, 2 (2012) 70-90.
- [40] M. Kurisawa, M. Terano, N. Yui, *J. Biomater. Sci. Polym. Ed.*, 8 (1997) 691-708.
- [41] M. Fan, Y. Ma, Z. Zhang, J. Mao, H. Tan, X. Hu, *Materials Science and Engineering: C*, 56 (2015) 311-317.
- [42] Y. Xin, J. Yuan, *Polymer Chemistry*, 3 (2012) 3045-3055.
- [43] C. Qian, T. Zhang, J. Gravesande, C. Baysah, X. Song, J. Xing, *Int. J. Biol. Macromol.*, 123 (2019) 140-148.
- [44] X. Peng, Q. Zhuang, D. Peng, Q. Dong, L. Tan, F. Jiao, L. Liu, J. Liu, C. Zhao, X. Wang, *Iran J Pharm Res*, 12 (2013) 581-586.
- [45] S. Wu, L. Deng, H. Hsia, K. Xu, Y. He, Q. Huang, Y. Peng, Z. Zhou, C. Peng, *J Biomater Appl*, 31 (2017) 1380-1390.
- [46] A.D. Pearle, R.F. Warren, S.A. Rodeo, *Clin. Sports Med.*, 24 (2005) 1-12.

- [47] R. Oettmeier, K. Abendroth, S. Oettmeier, *Acta Morphol. Hung.*, 37 (1989) 169-180.
- [48] E. Sukur, C. Talu, Y.E. Akman, E. Circi, Y. Ozturkmen, T. Tuzuner, *Acta Orthop. Traumatol. Turc.*, 50 (2016) 458-463.
- [49] L.A. Stoppiello, P.I. Mapp, D. Wilson, R. Hill, B.E. Scammell, D.A. Walsh, *Arthritis & rheumatology (Hoboken, N.J.)*, 66 (2014) 3018-3027.
- [50] H.V. Bonde, M.L. Talman, H. Kofoed, *APMIS*, 113 (2005) 349-352.
- [51] H. Muir, *Bioessays*, 17 (1995) 1039-1048.
- [52] T. Hardingham, M. Bayliss, *Semin. Arthritis Rheum.*, 20 (1990) 12-33.
- [53] Y. Sun, D.R. Mauerhan, J.S. Kneisl, H. James Norton, N. Zinchenko, J. Ingram, E.N. Hanley, Jr., H.E. Gruber, *Open Rheumatol. J.*, 6 (2012) 24-32.
- [54] G. Papacrhistou, S. Anagnostou, T. Katsorhis, *Acta Orthop. Scand. Suppl.*, 275 (1997) 132-134.
- [55] R. Bustos Latabán, I.A. Marino Martínez, V.J. Romero Díaz, O.F. Mendoza Lemus, J. Lara Arias, S. De La Garza Castro, *International Journal of Morphology*, 32 (2014) 1199-1206.
- [56] J.P. Pelletier, F. Mineau, J.P. Raynauld, J.F. Woessner, Jr., Z. Gunja-Smith, J. Martel-Pelletier, *Arthritis Rheum.*, 37 (1994) 414-423.
- [57] J.P. Pelletier, D. Lajeunesse, D.V. Jovanovic, V. Lascau-Coman, F.C. Jolicoeur, G. Hilal, J.C. Fernandes, J. Martel-Pelletier, *J. Rheumatol.*, 27 (2000) 2893-2902.
- [58] A. Naumann, J.E. Dennis, A. Awadallah, D.A. Carrino, J.M. Mansour, E. Kastenbauer, A.I. Caplan, *J. Histochem. Cytochem.*, 50 (2002) 1049-1058.
- [59] F. Nelson, L. Dahlberg, S. Lavery, A. Reiner, I. Pidoux, M. Ionescu, G.L. Fraser, E. Brooks, M. Tanzer, L.C. Rosenberg, P. Dieppe, A. Robin Poole, *J. Clin. Invest.*, 102 (1998) 2115-2125.
- [60] D. Pfander, R. Rahmanzadeh, E.E. Scheller, *J. Rheumatol.*, 26 (1999) 386-394.
- [61] Z. Zhang, X. Wei, J. Gao, Y. Zhao, Y. Zhao, L. Guo, C. Chen, Z. Duan, P. Li, L. Wei, *Int. J. Mol. Sci.*, 17 (2016) 411.

- [62] N. Bellamy, J. Campbell, V. Robinson, T. Gee, R. Bourne, G. Wells, Cochrane Database Syst. Rev., (2006) Cd005328.

Journal Pre-proof

CRedit author statement

Luis García-Fernández: Conceptualization, Methodology, Validation, Formal analysis, Investigation, Writing - Original Draft, Visualization

Marta Olmeda-Lozano: Methodology, Validation, Investigation, Writing - Original Draft

Lorena Benito-Garzón: Methodology, Validation, Investigation, Writing - Original Draft, Visualization

Antonio Pérez-Caballer: Conceptualization, Supervision, Funding acquisition

Julio San Román: Conceptualization, Resources, Supervision, Project administration, Funding acquisition

Blanca Vázquez-Lasa: Conceptualization, Resources, Writing - Review & Editing, Supervision, Project administration, Funding acquisition

Journal Pre-proof

Declaration of interests

The authors declare that they have no known competing financial interests or personal relationships that could have appeared to influence the work reported in this paper.

The authors declare the following financial interests/personal relationships which may be considered as potential competing interests:

Journal Pre-proof

Highlights

Osteoarthritis is a chronic degenerative disease that constitutes a public health problem

Semi-IPN hydrogels loaded with anti-inflammatory drugs are developed for drug delivery

Degradation/release profile of the hydrogels is anti-inflammatory drug dependent

Naproxen-loaded hydrogels avoid the progression of cartilage degeneration

Dexamethasone-loaded hydrogels allow cartilage regeneration and avoid osteoarthritis progression

Journal Pre-proof